



Investigation on the Gas Jet Flow Performance Confined in Round Pipe

H. Zhang¹, L. Jia^{1†}, L. S. Cui^{2†} and C. H. Li²

¹ *Beijing Key Laboratory of Flow and Heat Transfer of Phase Changing in Micro and Small Scale, School of Mechanical, Electronic and Control Engineering, Beijing Jiaotong University, Beijing 100044, China*

² *National Institute of Metrology, Beijing 100029, China*

†*Corresponding Author Email: ljia@bjtu.edu.cn; cuils@nim.ac.cn*

(Received May 19, 2020; accepted October 1, 2020)

ABSTRACT

In this study, the round jet flow behavior arose by the confinement was investigated experimentally and numerically. The confinement characteristics based on multi-scale characterizations in the atmospheric gas jet flow, which generated from a circular symmetrical subsonic nozzle and flowed into a confined round pipe, was used to be studied. The studied region near the nozzle possess really short axial length (within $12d$), providing initial conditions and boundaries that affected the flow behaviors in this region. A wide range of inlet velocities (0.98 m/s~84.72 m/s) and confined space sizes (1~20) were involved for simulated and quantitative discussions. The velocity profile evolution was recorded by simulations and characterized by a laser Doppler anemometer (LDA) with a resolution of 0.01 m/s. The confinement characteristics were systematically presented to elucidate the performance under the studied confined conditions with different metrics, such as centerline velocity decay (V_R), entrainment rate (M_R), pressure coefficient (C_p) and length of recirculation region (L_R). The results indicated that the recirculation fluid action mainly contributed to the promoted initial velocity profile evolution with the introduction of the confined space. Theoretically, the confined space could reduce the maximum absolute entrainment mass flux, initiating a peak at the center of the recirculation region, which was controlled by the inlet velocity and the confined space size collectively. The remarkable effect of confined space size further contributes to the confinement characteristics of gas jet flow, representing a shortened flow distance despite similar process as that by reducing the diameter ratio (d_R). In some cases, because of the miniaturization of confined space size, the dispersion of initial velocity profile evolution was not significant displayed throughout the variable inlet velocity range, especially when the d_R was less than 2. This study gives a new insight in the performance of jet flow confined in round pipe, and such knowledge will be helpful to provide great potential and reference to applied fluid mechanics.

Keywords: Confined jet; Confined pipe; Confinement characteristics; Size effect.

NOMENCLATURE

C_1, C_2	in $k-\varepsilon$ turbulence model	p_0	reference static pressure
C_p	pressure coefficient	p_w	wall static pressure
C_u	empirical constants appearing	q_0	gas flow flux at nozzle exit
d	exit diameter of contraction nozzle	Q_0	jet exit volume flow rate
D	entrance diameter of contraction nozzle	q_i	gas flow at different axial positions
d_R	diameter ratio of confined space	Q_i	jet streamwise volume flow rate
H	diameter of confined space	u_0	inlet velocity/centerline velocity at nozzle exit
K_1, K_2	constant parameter	u_c	centerline velocity
L	length of confined space	V_R	centerline velocity decay
L_R	length of recirculation region	X	streamwise coordinate
L_S	length of contraction nozzle	Y	vertical coordinate
m_0	jet exit mass flow rate	ν	kinematic viscosity
m_e	jet excess mass flow rate	ρ	density
m_j	jet streamwise mass flow rate		
M_R	entrainment rate		
p_0^*	reference total pressure		

1. INTRODUCTION

Jet flow is a typical flow regime in turbulence and has been increasingly used to achieve the exchange of momentum, heat transfer and mass. Generating from a source and flowing to a quiescent environment, it can be classified into a free jet and confined jet, which depends on whether the downstream is surrounded by an infinite or a confined space (Schlichting 2000). The presence of confined walls induces a recirculation region in the confined space which promotes a more rapid evolution of the jet flow (Ahmed *et al.* 2000). Thus, the confined jet is usually treated as a kind of effective active flow controller based on the change of downstream confined space (Cattafesta *et al.* 2011), which has potential applications in measurement, industry, aerospace and other related fields, such as the measurement of gas flow in large-scale pipe (Zhang *et al.* 2019), the enhance cooling (Jiang *et al.* 2016) and jet pump (Sheha *et al.* 2018; Chang *et al.* 2020).

The initial velocity profile evolution of a confined jet would contribute much to the applications mentioned above. Particularly, some special behaviors of the initial velocity profile evolution occur within a confined jet in variable confined spaces, involving the length of potential flow, entrainment rate (M_R), mixing performance, etc. Some theoretical formulas were proposed based on the regular and constant confined space in order to predict the M_R (George *et al.* 1988; Hussein *et al.* 1994). Yang *et al.* (2012) numerically studied a coaxial confined jet in a round pipe with an area ratio of 11.28, using high-temperature compressible flow of 130 °C as the working fluid. It indicated that the efficient mixing was improved by the special geometry of confined space and an increasing nozzle exit perimeter, induced by the enhanced mixing shear layer between the two coaxial flows. Deo *et al.* (2007) experimentally studied the centerline velocity decay (V_R) of confined jet with sidewalls and found that the longer length of potential flow and the decreased decay were attributed to the presence of the confined sidewalls. In order to explore the underlying mechanisms for the special behaviors, many investigations about the initial velocity profile evolution of confined jet were conducted experimentally and numerically.

The study on the recirculating fluid behaviors is the key to fully understand the initial velocity profile evolution of confined jet. The multi-scale recirculation region is the topical flow pattern in the confined jet resulted from the miniaturized downstream space, which could promote the evolution of confined jet. Morris *et al.* (1999) numerically studied the evolution of an impinging confined jet and found that the inlet velocity has a significant positive influence on the mixing interaction between the recirculation region and jet. Sheen *et al.* (1996) experimentally investigated the recirculation region behind the cylindrical bluff

body of a coaxial confined swirling jet. They proposed that the recirculation region length increased linearly with a critical inlet velocity and then turned into a negative exponential relationship. The critical inlet velocity changed with the increasing swirl number, which revealed a dominant factor exactly lying in the effect of the confined space on the recirculation region (So *et al.* 1985). Fitzgerald *et al.* (1997) experimentally observed the center of the recirculation region moving away from the nozzle with the increased inlet velocity. Razinsky and Brighton (1971) firstly explored the effect of confined space size on the mixing of coaxial confined jet utilizing the diameter ratio (d_R) and it was emphasized that the initial velocity profile evolution of the confined jet generated from the near field and reach the fully developed region.

The initial velocity profile evolution of a confined jet has a significant potential and referential on the achieved performance in variable applications, and the mixing process and entrainment behavior account for the main embodies of the evolution, which exhibits the characteristics corresponding to different downstream confined conditions. From the mentioned literatures above, most studies investigated the increased mixing process achieved by enhancing recirculation region in different confined jet. However, limited studies gave priority to the confined space as the dominant influencing factor wherein the diversity of the confined space structures also gives difficulties in proposing universal formulas.

Moreover, due to the unique and stable velocity profile near the nozzle, the parameters of round confined jet play the key role in the velocity-area method when applied in the gas flow measurements (Mickan and Strunck 2014). Primarily in this procedure, the measured flow is obtained by integrating the velocity profile near the upstream nozzle, which further introduces differences between the measured value and the real value caused by the initial velocity profile evolution of the confined jet. Nevertheless, the confined evolution of the initial velocity profile still needs to be fully described compared to the studied mixing, which involved the V_R and M_R . What's more, from an unconfined state to a deeply confined state, the way by which the evolution gradually transforms is not fully understood as well, especially for the region near the nozzle. Therefore, to improve the achieved performance of the initial velocity profile evolution of a confined jet, an evolution mechanism and the effect of confined space size are required.

In this work, the confined evolution of the initial velocity profile was studied from a circular symmetrical nozzle into a confined round pipe by multi-scale characterizations. Eliminating the effect of the space with variable cross-section on the confined evolution contributes to the understanding of the essential synergistic relationship among the confined evolution of initial velocity profile, recirculation region behavior, and confined space

size. In this study, the confined jet was experimentally studied by the jet flow standard facility in the Chinese National Institute of Metrology (NIM). The d_R of confined space was 4 and 1.73 and the inlet velocity was from 0.62 m/s to 43.41 m/s. The confined jets flowed into multi confined spaces with different inlet velocities (0.98 m/s-84.72 m/s) were analyzed in details based on numerical simulations.

2. EXPERIMENTAL AND NUMERICAL SCHEMES

2.1 Experimental Apparatus

Figure 1 provides a schematic diagram of the jet flow standard facility used in this study within atmospheric air as the working fluid. The round jet was generated by the pressure difference when the jet flows through the contraction subsonic nozzle into a confined space. The nozzle has a smooth shrinkage in diameter from 200 mm (D) to 66.7 mm (d) and the specific geometric parameters of the confined space are described in section 2.2. The pressure difference was generated by an invariable frequency roots vacuum pump and the entire range of inlet velocity (0.62 m/s-43.41 m/s) matched with the sonic nozzle bank by controlling the opening of six sonic nozzles with different throat diameters. The confined jet investigated here with an enough inlet straight duct (2400 mm long with a 200 mm diameter bore) had a good approximation to an axisymmetric initial velocity profile (Hussein *et al.* 1994).

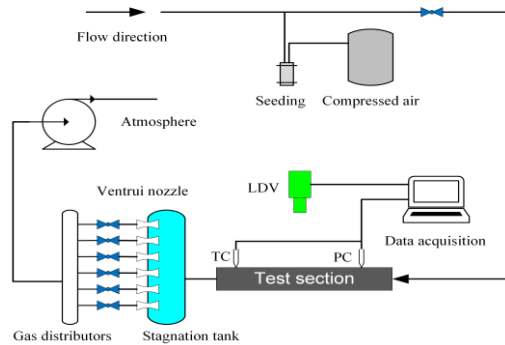


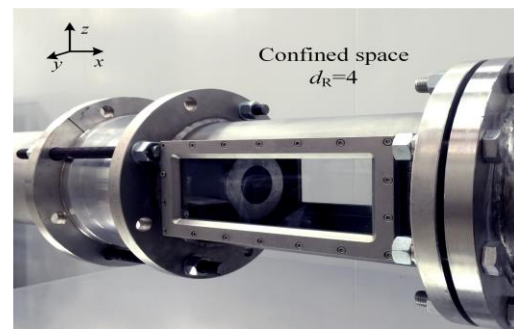
Fig. 1. Schematic diagram of the jet flow standard facility.

A two-dimensional LDA (Dantec Firbe Flow P60) with a resolution of 0.01 m/s was utilized to measure the round jet in the confined space. The measurement volume was formed by interference of two homologous laser beams (532-nm wavelength pulsed laser) and a seeding generator (Dantec 10F03 with 5 μ m particles seeding) was located before the inlet straight duct to provide enough tracing particles for it. The LDA was mounted on a automatic traversing system that allowed motion in three directions with resolutions of 0.01 mm in every direction. High precision pressure gauges with uncertainties of

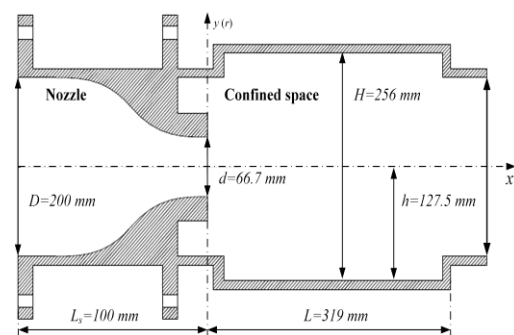
0.01% of the span were used to measure the differential pressure between the inlet and the outlet of nozzle and the absolute pressure in confined space. Temperature was measured with PT-100 platinum resistance with the total uncertainties of 0.02%. All measuring instruments in the study were calibrated by NIM and the uncertainty of measured jet velocity was about 0.2% (Zhang *et al.* 2019).

2.2 Confined Space

The test section and the confined space are the core parts in the study, as shown in Fig. 2, which can be regarded as an essentially cylinder with coaxial confinement. One of the internal dimensions was 319 mm \times 267 mm ($d_R = 4$) \times 200 mm. Another was 160 mm \times 100 mm ($d_R = 1.73$) \times 100 mm. The glass windows on both sides of the confined space were designed to meet the requirements of optical measurements. The basic experiments were based on the above geometric model. In order to determine clear correlations corresponding to the effect of confined space on the near behavior of the confined jet, more confined structures with the same contraction nozzle but variable diameter were studied by CFD as shown in Table 1.



(a): basic structure



(b): specific parameters

Fig. 2. A confined space ($d_R = 4$) with glass optical windows within the confined jet flowing through.

2.3 Modelling and Mesh

Figure 2 presents the physical model of the test section in this study. The numerical models shared the same geometric parameters. In order to avoid backflow, the downstream of straight duct was

Table 1 Numerical simulation parameters for different confined spaces

Contents	Range									
$H/d (V_R)$	1	1.2	1.5	2	2.5	4	5	8	10	20
H/L	0.067	0.08	0.1	0.133	0.167	0.267	0.333	0.533	0.667	1.333
Mesh number ($\times 10^5$)	6.469	4.196	4.256	4.319	4.566	5.922	5.933	5.993	6.086	8.021
Mass flow flux (kg/s)	0.0045-0.3804									
inlet velocity (m/s)	0.98 - 84.72									

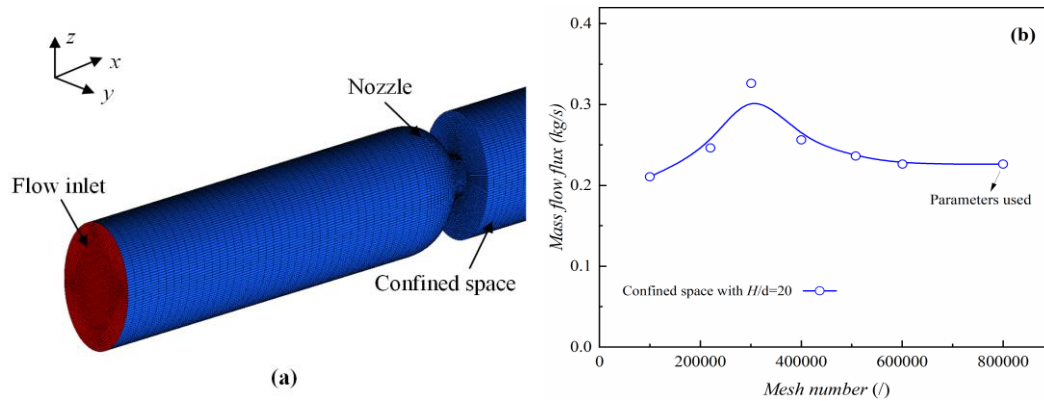


Fig. 3. (a) The geometry and mesh at $V_R = 4$; (b) The grid independence verification at $d_R = 20$.

extended for $L = 15d$ and the overall length of the model was about 2200 mm. The diameter of confined space changed according to the d_R . Table 1 presents the parameters applied in mesh generation. Three-dimensional structured grids were used and it meshed by ICEM. The base size was 2 mm. The prism layers were 5 and the ratio was 1.1. The grid from the nozzle entrance to the confined space was densified to improve the quality of the calculation. The grid independence behavior was used to verify the applicability of the selected grid parameter shown in Fig. 3.

2.4 Numerical Scheme

The numerical simulation was performed using the mature commercial simulation software package, FLUENT R19.2, with a solver based on pressure and steady time. The flow governing equations were set up based on the three-dimensional Navier-Stokes equations for a viscous incompressible ideal gas, of which the density was calculated using the ideal gas state equation. The standard k -epsilon turbulence model and enhance wall treatment were adopted to calculate the steady state as its excellence predictive performance for coaxial confined jet (Yang *et al.* 2012). The turbulence model used the recommended empirical factors $C_{mu} = 0.09$, C_1 -epsilon = 1.44 and C_2 -epsilon = 1.92. SIMPLE method was used for the coupling of fluid velocity and gas pressure. At the time, momentum turbulence kinetic energy and turbulence dissipation rate were second order upwind.

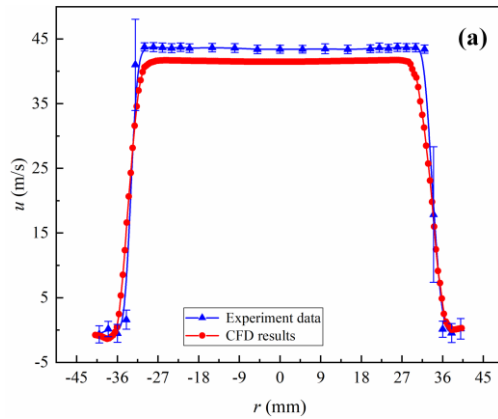
The boundary conditions were confirmed according to the experimental conditions to ensure that the numerical model was reasonable and approximate

to the actual situations. The confined space possessed a solid wall of aluminum, which provided an adiabatic and non-slip boundary, within the air acted as the fluid flowing through it. Therein the inlet pressure, as the entrance condition, and the outlet pressure, as the exit condition, were close to the working pressure of vacuum pump. The fluid temperature was 291.15 K and turbulence intensity was determined as 0.3%.

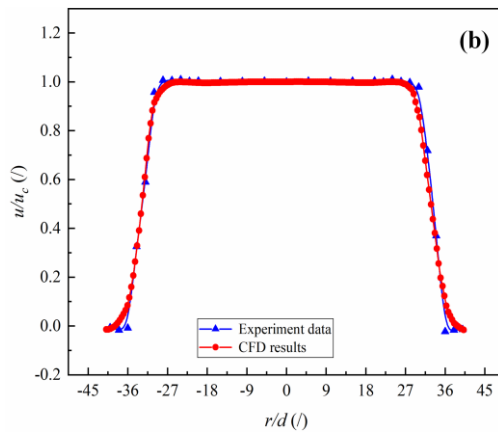
2.5 Numerical Simulation Validated by Experiments

Figure 4 shows the validation results of numerical simulation by experiments at two jet exit velocities. The numerical simulation was carried out for the confined space with $d_R = 4$, which was nearly consistent with the size of the confined structure used in the experiment. It showed that the top-hat profiles distribute with the saddle back in core flow part wherein the difficulty of numerical simulation lied in the boundary layer flow. The numerical code was properly validated for low velocity below 43 m/s due to the systematic limitation. Note that the influence of boundary layer flow would decrease with the increase of velocity, and this design was enough for validating that of high velocities.

During testing, the discrepancy originated from the inaccurate discharge coefficient of sonic nozzle induced a certain but limited deviation between ideal and real mass flow. Thus, at the inlet velocity of 43 m/s, the difference in average velocity would directly cause a slightly lower calculated inlet mass flux than the reality. In general, the simulation results showed good agreement with that of the experiments.



(a) $u_c \approx 43$ m/s



(b) $u_c \approx 2$ m/s

Fig. 4. Comparison of the normal top-hat velocity profile near nozzle between numerical and experimental results for the confined space with $d_R = 4$.

3. RESULTS AND DISCUSSIONS

In order to quantitatively analyze the round jet flow behaviors confined in the round pipe, originating from published papers (Hussein *et al.* 1994; Schlichting 2000; Zhang *et al.* 2019) and considering the specialty in this work, two non-dimensional parameters referring to the V_R and M_R were defined as:

$$V_R = \frac{u_c}{u_0} \quad (1)$$

$$M_R = m_e/m_j = (m_j - m_0)/m_0 = Q_j/Q_0 - 1 \quad (2)$$

where u_c is the local centerline velocity and u_0 is the centerline velocity at nozzle exit; m_e is the excess mass flow rate of the jet; m_j , Q_j are the streamwise mass flow rate and streamwise volume flow rate of the jet respectively; m_0 , Q_0 are the jet exit mass flow rate and jet exit volume flow rate respectively; The V_R and M_R represent the length of potential flow and the evolution speed of initial velocity profile, respectively, which are deeply associated with the inlet velocity u_c .

On this basis, the effect of the confined space size on the confinement characteristics of studied confined jet was discussed in details. The confined space size was also characterized by a non-dimensional parameter d_R , named as the diameter ratio of the test confined pipe. It was defined as (Razinsky and Brighton 1971):

$$d_R = \frac{H}{d} \quad (3)$$

The studied region (with an axial length of $12d$) located in the near field or intermediate field of jet flow, simplified, seems not sufficient to adapt to a full development. Nevertheless, in fact, the flow behaviors were indeed closely affected by the initial conditions and boundaries of the near field and intermediate field, providing higher referential significance to different engineering applications (Ball *et al.* 2012). In addition, the specific length of the studied region was actually related to the d_R of confined space and all was located upstream far field. So, the research emphases lied in the studied region with small axial lengths.

With the aim of elucidating the effect of inlet velocity u_c and confined space d_R on the parameters mentioned above, the following discussion were addressed.

3.1 The Jet Flow Performance Confined in Round Pipe

Previous studies implied that the addition of confined space could influence the round jet behaviors in the near field, hence the difference between them was discussed (Ball *et al.* 2012). The studied round jet was confined in a constant downstream space with $d_R = 4$ in this section. The constant d_R made it possible to simply study the initial velocity profile evolution of confined jet at different inlet velocities without the noise from variable confined space. As a common confined condition in previous literatures, the constant d_R was also a suitable value to describe both the unconfined state and the deeply confined state in this research.

Several results of V_R corresponding to different confined conditions in some well-established publications were shown in Fig. 5 (Abdel-Rahman *et al.* 1996; Kwon *et al.* 2005; Suresh *et al.* 2008). For the round jet, the V_R increased more significantly in the confined space, indicating a promotion of the V_R caused by the confined space. For the confined jet, V_R was found to be closely related to the special confined structure. In round free jet, the V_R depended directly on the flow pattern of vortex structure in the mixing region, which possessed a process including formation, advection and diffusion corresponding to the duration of transition from laminar to turbulence by changing initial velocity. Differently, the recirculation region in confined space which originated from the presence of confined structure can also influence it. Therefore, the coupling effect of confined space and inlet velocity on round jet

behavior is worthy of further discussion.

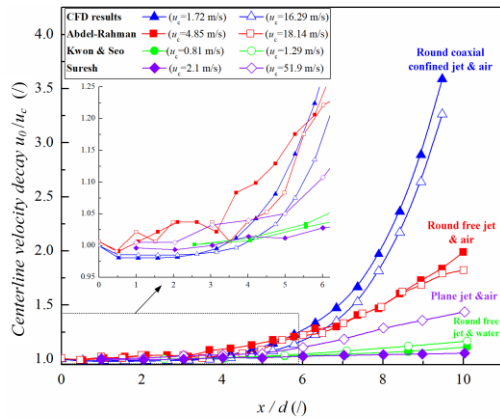
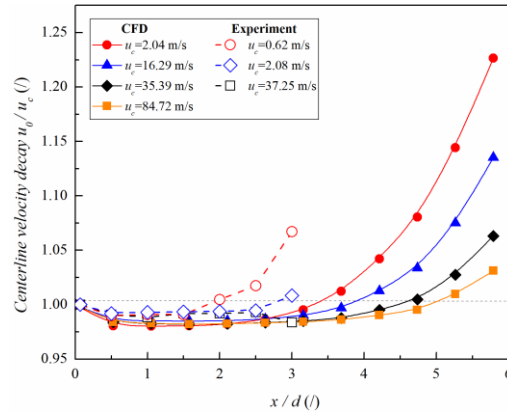


Fig. 5. Comparison of centerline velocity decay (V_R) between the present results and the previous literatures.

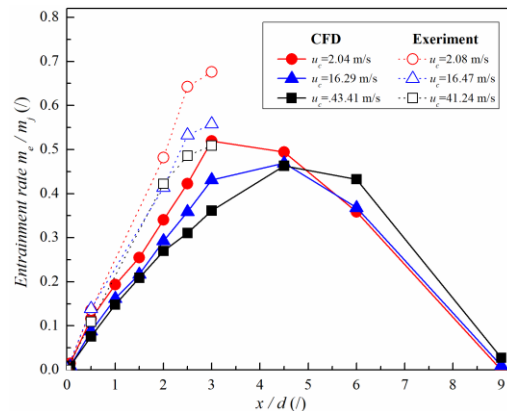
The V_R and M_R in the work resulted from the studied confined jet at wider range of inlet velocities are shown in Fig. 6. The range of the inlet velocity was from 0.62 m/s to 84.72 m/s, therein the range from 0.62 m/s to 41.24 m/s was verified by experiments. The expanded inlet velocity range corresponded to the gas flow range of about 10 m³/h -1000 m³/h under the constant nozzle exit diameter, which was basically held responsible for the measurement capacity of different flowmeters below Dn 200.

Along the flow direction, the V_R exhibited a sharp increase at the beginning, illustrating as a value of V_R decreased rapidly below 1 in Fig. 6 (a). Then the increasing rate turned to be smooth after $0.5d$ for a certain distance, following by a gradually decrease of the centerline velocity. This indicated that the evolution of initial velocity profile near the nozzle was mainly driven by the recirculation region as well as the expansion effect. The acceleration of the decrease of expansion effect induced by the positive pressure gradient and the obvious interaction with the surrounding gas occurred simultaneously, which indicated that the onset of the V_R occurred after the value of V_R was greater than 1. The experimental data was slightly higher than the simulation results in absolute value of the ratio, since the starting point of the measurement was only close to the exit. The measured value u_0 was increased by the expansion effect, while it was unrelated to the curves of experiments and simulations which shared a similar evolution trend. The local performance of V_R depended on the recirculation region behavior, which varied with inlet velocity and continued until the width of confined jet reached the confined space wall with the disappearance of recirculation region. The confined jet was fully confined by the space wall in its radial direction at that moment, hereafter the fluid restored to pipeline flow. In addition, it should be noted that there was a coupling effect between the time average feature mentioned above and instantaneous vortex shedding behind the bluff

body of vertical confined space wall during V_R process near the nozzle. With the coincidence of the acceleration of the decay started and the increase of inlet velocity, the curves were slowly independent to the inlet velocity. This coupling variations between two confined evolution parameters persisted until the inlet velocity was fully higher than a critical value which was related to the special confined condition.



(a) Centerline velocity decay (V_R)

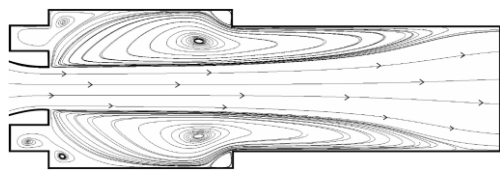


(b) Entrainment rate (M_R)

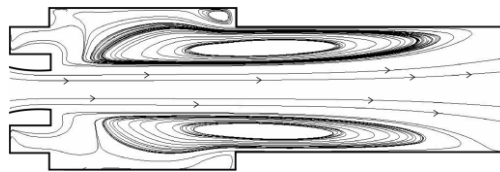
Fig. 6. Variations of confined flow characteristics evolution of confined jet in constant confined space $d_R = 4$.

The variation features of M_R in the constant confined space could further expose the evolution speed of initial velocity profile of confined jet. The M_R increased rapidly and reached a peak at around the middle of flow distance, then turned to a subsequent decrease, which distributed as an inverted V-shape in the whole process showed in Fig. 6 (b). This was different from the linear growth in round free jet (Ball *et al.* 2012). The inverted V-shape distribution of the confined jet also implied that the evolution of the initial velocity profile in the whole process was mainly attributed to the recirculation region. Some surrounding gas was used to preserve the recirculation region driven by the adverse pressure gradient, and the other was drawn into the confined jet, which enhanced the momentum loss and accelerated the evolution of initial velocity profile. The reinforcement of the

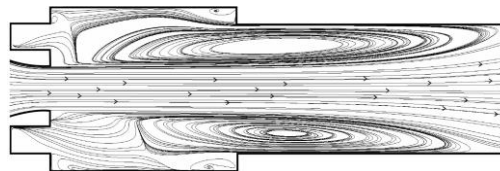
recirculation region raised firstly and followed by a decrease along the flow direction, of which the maximum adverse pressure gradient appeared at the center of recirculation region. Note that the peak of M_R directly referred to the center of recirculation region and the location of the peak moved upstream as decreasing of inlet velocity, which was special for the corresponding recirculation region. The experimental results were also slightly higher than that of the simulations due to the lower calculated inlet mass flux, which was used as the Q_0 for the experiments. Furthermore, the coupling effect between the time average feature and instantaneous vortex shedding mentioned above was more obvious in the M_R evolution of confined jet, which indicated that the faster M_R measured by experiments at the lowest inlet velocity after $0.5d$.



(a) $u_c = 2.08$ m/s



(b) $u_c = 19.52$ m/s



(b) $u_c = 84.72$ m/s

Fig. 7. Development of recirculation regions in confined jet with increasing inlet velocity ($d_R = 4$).

Thus, the initial velocity profile evolution of confined jet involved remarkable role of recirculation region in the process. In order to discuss the recirculation region in details, the non-dimensional parameter pressure coefficient (C_p) based on the previous literature (Ötügen 1991) was re-defined as:

$$C_p = \frac{P_w - P_0}{P_o^* - P_0} \quad (4)$$

where p_o^* , p_0 are the reference total pressure and static pressure, which are obtained at $y = -d/2$; P_w is the wall static pressure obtained at $y = -D/2$, a baseline chosen from downstream step to exclude the possible effect of the special confine space. C_p represents the relative pressure gradient between the

confined jet and surrounding gas at the same axial location, and the negative value indicates that the recirculating fluid is more likely to occur. The step-side wall static pressures were obtained for various inlet velocities. The resulting C_p was shown in Fig. 7. The larger-scale recirculation region resulted from the continuous negative pressure coefficient was found in the downstream confined space.

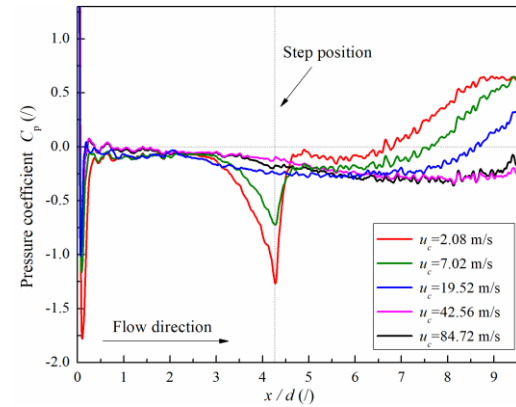


Fig. 8. Variations of C_p in the confined jet ($d_R = 4$).

As can be seen in Fig. 8, the steep drop of C_p near the nozzle exit indicated the beginning of initial velocity profile evolution of confined jet. This flow separation at the nozzle outlet resulted in the suddenly increased static pressure p_0 without nozzle walls and then decreased, leading to a peak of pressure. Meanwhile, the outside fluid velocity of the confined jet suddenly increased at first, then turned to be slowly wherein the initial velocity profile gradually evolved from the outside to the centerline along flow direction. Another trend evident in the C_p results was that the higher inlet velocity led to the faster development of pressure with shorter distances from the separation position to the location of minimum C_p . The disappearance of nozzle wall caused increased viscous shear force which related to the strongly interaction between surrounding gas and the formed jet. This was coupled with expansion effect to induce the faster development of pressure, indicating the fastest evolution of V_R and M_R near the nozzle. Due to the expansion effect, the C_p recovered and fluctuated until it dropped again. This was reflected before $2d$ in Fig. 8, which also referred to the slow growth stage of V_R mentioned above. Therefore, C_p was the dominate factor for the recirculation region which reinforced the initial velocity profile evolution. The expansion effect promoted the special trend of C_p , which varied with inlet velocities in a constant confined space.

It should be noted that the second peak in Fig. 8 was a special characteristic of the studied confined space with the downstream step. The diameter of the confined space suddenly reduced and the wall static pressure increased faster under the role of the viscous force, which caused the C_p increased from negative to positive. This also strongly illustrated

that the confined space size had a significant influence on C_p compared to the inlet velocity. It was also worthy to note that the zero point of C_p after the second peak moved downstream with the increasing inlet velocity, indicating a moved center of recirculation region, since a longer development distance was needed when the reversal point formed a recirculation region.

C_p after processing was more representative to the evolution of initial velocity profile and more effective to get the recirculation region behaviors. According to the C_p results as shown in Fig. 8, C_p developed asymptotic to a similar distribution with the increase of inlet velocity. The region was located at the downstream of the nozzle more than ten times the diameter which was far less than $70d$. This showed that the addition of the confined space can effectively shorten the length of near field. The effect of the inlet velocity on the round confined jet becomes weaker as it increased, and the confined jet was independent of the inlet velocity above 42.56 m/s under the studied conditions, which was related to the recirculation region in the confined space.

As a whole, present results indicated that the adverse pressure gradient in the additional confined space acted as the main reason for the formation of the recirculation region, and interacted with the expansion effect to enhance the initial velocity profile evolution of the confined jet, both in V_R and M_R . The increase of the inlet velocity could improve the uniformity of C_p in the confined space, promoting the recirculation region performance and the initial velocity profile evolution. On the other hand, the reduction of the confined space size could affect the recirculation region performance and it will be discussed in detail later. These aspects corresponding to the addition of the confined space made the confined jet attractive candidates for near field applications which was applicable to the requirements of gas flow measurements.

3.2 The Effect of Confined Space Size

The initial velocity profile evolution of the confined jet was related to not only the inlet velocity but also the size of confined space, which was attributed to the recirculation region performance and expansion effect. The initial velocity profile evolution of confined jet was studied at different downstream confined conditions by changing d_R . The studied range of d_R was from 1.2 to 20, and $d_R = 1.73$ as well as 4 was verified by experiments. The expanded d_R range corresponds to the inlet velocity range was basically held responsible for the application requirements of gas flow measurement based on the velocity-area method. The variations of local performance of recirculation region at different confined conditions during evolution processes were shown in Fig. 9.

As can be seen in Fig. 9, larger d_R led to the slightly increased the length of recirculation region (L_R) and the distance to nozzle exit, resulting in the change of initial velocity profile evolution of confined jet at different confined conditions. It could be attributed to the enlarged d_R promoting the continuous distribution

of negative pressure coefficient, which was more conducive to the emergence and development of the recirculation region. Similar to the effect of the inlet velocity, the behavior of recirculation region was gradually independent on the increasing d_R , indicating that there was a critical confined condition for the initial velocity profile evolution of the confined jet. However, compared with the confined jet of $d_R = 4$, the confined jet of $d_R = 8$ revealed different rules. It was evident that downstream step resulted from a limited length of the confined space could lead to the slightly shorter normalized length and distance of recirculation region. Increasing d_R with limited length of the confined space caused the pressure at the step point which could produce the recirculation region but was lower than the pressure at the enlarged confined space wall. The recirculation region could be separated into two small-scale recirculation regions, and the scale near the centerline was larger, which undoubtedly affected the local performance of the recirculation region.

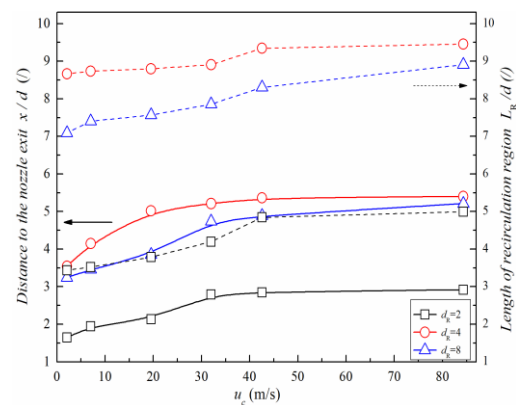


Fig. 9. Variations of the shape parameters of recirculation region during round jet developing in confined spaces.

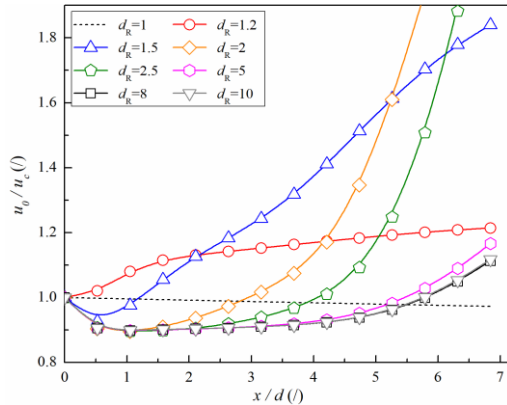
Considering the determinative of the analytical results to the pure annular confined jet without swirl, L_R and related formula in a constant confined condition was given (Sheen *et al.* 1996), which gave a reference to compare the local performance, expressed as:

$$L_R/d = K_1 u_c d / \nu \tag{5}$$

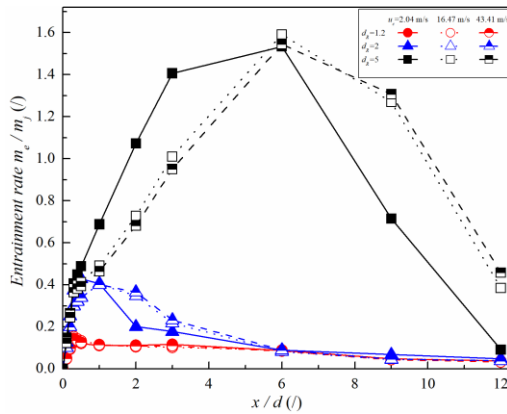
$$L_R/d = K_2 + \nu / K_1 u_c d \tag{6}$$

Where K_1 and K_2 are the constant parameter. The former is used at Reynolds numbers less than 300 and the latter is used at higher Reynolds numbers. It was apparent that the inlet velocity contributed to the recirculation region at constant confined condition. However, the size of the confined space is the dominate factor compared to the inlet velocity, as K_1 and K_2 are sensitive to the confined conditions. It was noticed that L_R increased nonlinearly with the increasing inlet velocity, which was related to the unsteady vortex-shedding. This was consistent with the findings in this research, wherein the round confined jet was in a

confinement state with recirculation region. Therefore, more detailed discussions about the effect of confined space size would be carried out for the evolution referring to V_R and M_R corresponding to the recirculation region performance.



(a) Centerline velocity decay (V_R)



(b) Entrainment rate (M_R)

Fig. 10. Variations of confined evolution of round jet confined in different spaces.

The variations of V_R with different confined spaces at $u_c = 57.54$ m/s are shown in Fig. 10 (a). Comparing the V_R of the confined jet in different confined spaces, the onset of V_R advanced and enhanced with the decrease of confined space size at a same inlet velocity. When $d_R > 5$, there was no obvious confinement effect of confined space on V_R , which was different from V_R in smaller confined space at the same inlet velocity condition. The distance of recirculation region to nozzle exit and the length of it were almost independent from the enlarged d_R with the increase of inlet velocity compared to smaller confined space. When $1 < d_R < 5$, the recirculation region was pushed to the nozzle exit timely with the decreased d_R , leading to the advance of the velocity decay. The velocity decay occurred at $x = 0.2d$ when the d_R decreased to $d_R = 1.2$, and the expansion effect region near the nozzle exit as well as the developing region of confined jet in the confined space was relatively short. When the d_R decreased to 1 without the confined jet, the confinement characteristics in it cannot occur.

Figure 10 (b) shows the variations of M_R with different confined spaces. All of the results indicated that the confined evolutions of the initial velocity profile gone through the process from jet flow to pipe flow, as mentioned above. The difference was that reducing the d_R could significantly advance and limit the stable degraded process from the peak value as well as the effect of inlet velocity on the degradation. In addition, the variations of the peaks at different inlet velocities enlarged with the increase of d_R . The entrainment behavior was strongly dominated by the recirculation region, which was the same as the V_R . When the d_R decreased, the recirculation region moved upstream timely with the enlarged space, reducing the dispersion of entrainment curves. Comparing the entrainment curves in different confined spaces, the proportion of M_R confined growth in its total growth period decreased with the smaller confined space. The confined peak appeared later in relatively large confined space in which the recirculation region could be more easily enlarged than in the small confined space. As the special behavior near the nozzle in the constant space, the effect of the confined space on the initial velocity profile evolution of the confined jet in the region was concerned.

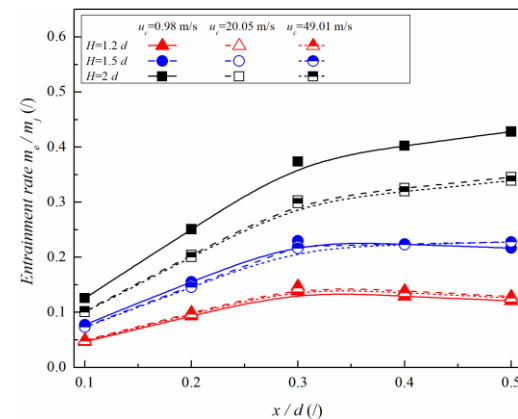


Fig. 11. Variations of M_R in the very near region of confined jet.

Figure 11 shows the variations of M_R with different confined spaces at variable inlet velocities near the nozzle. The distance was from the exit to $0.5d$ and the d_R was from 1.2 to 2. In very near region, all of the results increased rapidly at first and then tend to be gradual. At $d_R = 2$, there was obvious difference about 1% during the increasing inlet velocity, which was different from the other confined jet with smaller d_R at the same inlet velocity. As the d_R decreased below 1.5 with a difference less than 0.2%, which was corresponding with the limited action of recirculation region as shown in Fig. 9. As mentioned above, M_R was influenced by the jointly effect of recirculation region, vortex shedding and expansion effect to a more complicated extent, comparing with that in the further region. Reducing the d_R of the confined space not only constrained the recirculation region performance, but also needed to determine its influence on the vortex behavior. The time-average vorticity could be used

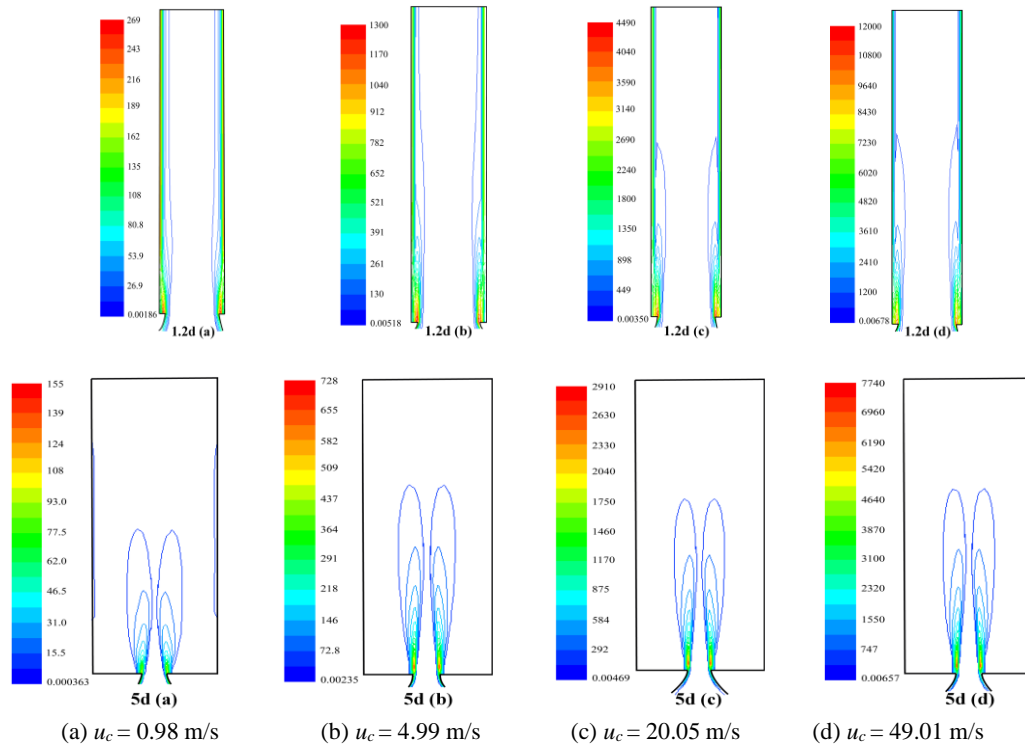


Fig. 12. Variations of vorticity contours of confined jet near nozzle exit ($d_R = 1.2$ and $d_R = 5$).

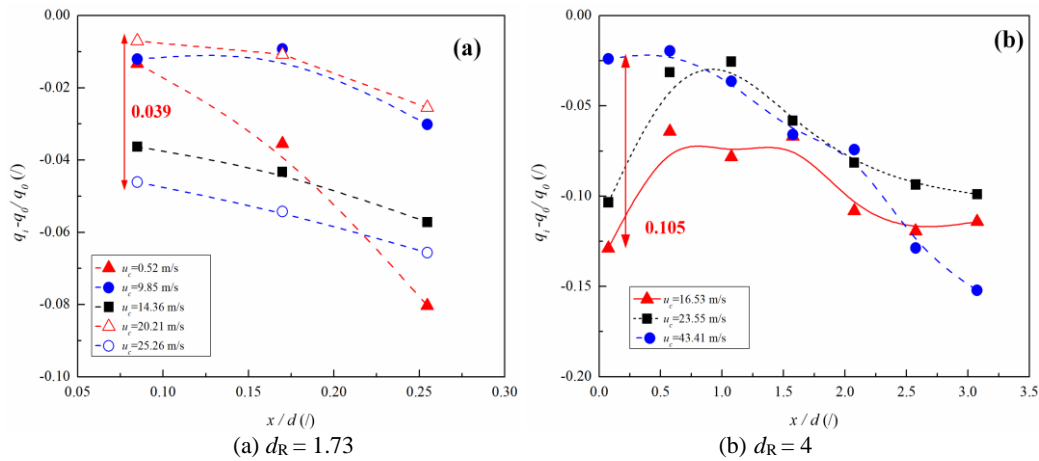


Fig. 13. Experimental verification of M_R affected by confined spaces.

to analyze the vortex intensity (Sheen *et al.* 1996), as shown in Fig. 12. It was evident that the vortex intensity was not strongly related to the reduction of confined space and the interaction between the vortex and surrounding gas was significant limited. The vortex was mainly in the mixing layer of the confined jet and the intensity increased with the increasing inlet velocity. Surrounding fluid on both sides of vortex region enlarged at high d_R of confined space, which brought higher entrainment compared with that at lower d_R . The dispersion of entrainment with different inlet velocities enlarged at the larger confined space.

On this basis, experimental verification of M_R affected by confined space was conducted by two

confined jets applied in gas flow measurement. The different results of the deviation (q_i was measured volume flux at different axial positions and q_0 was at the nozzle exit) (Mickan and Strunck 2014) are shown in Fig. 13. At $d_R = 1.73$, the observed dispersion was about 3.9% within $0.1d$, which was about 7% lower than in the confined space with $d_R = 4$ at a similar inlet velocity. Based on the improving consistency of measurement objects, reducing absolute variation could be achieved by a decreasing confined space. At $d_R = 4$, the deviation was closer to zero at higher inlet velocity within $0.5d$ from the distance to nozzle exit compared to other lower initial velocity. The experimental results further verified the above analysis that reducing d_R could limited the initial velocity profile

evolution of confined jet.

Thus, the initial velocity profile evolution of the confined jet was mainly attributed to the d_R of the confined space compared with the inlet velocity. Reducing the d_R could restrain the appearance and performance of recirculation region and relax the interaction between the confined jet and the surrounding gas, so as to promote the consistency of M_R at different inlet velocities. Nevertheless, it would also enhance the V_R and shorten the length of the core flow. Note that the critical value of the d_R was 2, by which the initial velocity profile evolution of confined jet was obviously independent of the inlet velocity in a smaller confined space.

5. CONCLUSIONS

In this work, the round jet flow performance due to the confinement of round pipe was investigated experimentally and numerically. A wide range of inlet velocities (u_c) from 0.98 m/s to 84.72 m/s and the diameter ratios (d_R) of studied confined space from 1 to 20 were simulated and quantitatively discussed. The axial length of the studied region was within $12d$, which was closely affected by the initial conditions and boundaries. Centerline velocity decay (V_R) and entrainment rate (M_R) resulted from the evolution of initial velocity profile are important for the confined jet, which is deeply related to recirculation region behavior in the confined space. All of the different metrics are associated with the downstream confined conditions including u_c and d_R . The following specific conclusions can be drawn based on the present study:

- (1) The addition of the confined space can significantly promote the initial velocity profile evolution by the formation of recirculation region, but it reduces the maximum absolute entrainment mass flux. The increased inlet velocity can change the initial velocity profile evolution, significantly influencing the pressure coefficient (C_p) in confined space and the local performance of recirculation region, which become more striking for the inlet velocity above 42.56 m/s under the studied conditions.
- (2) The remarkable effect of downstream confined space mainly further contributes to the confinement characteristics of gas jet flow, representing a shortened flow distance despite similar process by reducing the d_R . It owes to the weaker recirculation region induced by the change of C_p distribution in the confined space. Moreover, reducing confined space can also eliminate the dispersion of initial velocity profile evolution at different inlet velocities, especially when the d_R is less than 2.

ACKNOWLEDGEMENTS

This research was supported by The National Key Research and Development Program of China (No.2017YFF0205305).

Conceptualization, Han Zhang, Li Jia and Lishui Cui; Investigation, Han Zhang, Li Jia and Lishui Cui; Writing – original draft, Han Zhang; Writing – review & editing, Li Jia, Lishui Cui and Chunhui Li.

The authors declare no conflict of interest.

REFERENCES

- Abdel-Rahman, A. A., S. F. Al-Fahed and W. Chakroun (1996). The Near-Field Characteristics of Circular Jets at Low Reynolds Numbers. *Mechanics Research Communications* 23(3), 313-324.
- Ahmed, M. R., S. D. Sharma and Y. Kohama (2000). Experimental Investigation on Turbulent Mixing Enhancement in Confined, Co-axial Jets Using Chute Mixer Configuration. *JSME International Journal* 43(3),414-426.
- Ball, C. G., H. Fellouah and A. Pollard (2012). The Flow Field in Turbulent Round Free Jets. *Progress in Aerospace Sciences* 50, 1-26.
- Cattafesta, L. N. and M. Sheplak (2011). Actuators for Active Flow Control. *Annual Review of Fluid Mechanics* 43(1), 247-272.
- Chang, H., W. Shi, W. Li, C. Wang and K. A. Ramesh (2020). Experimental Optimization of Jet Self-Priming Centrifugal Pump Based on Orthogonal Design and Grey-Correlational Method. *Journal of Thermal Science* 29(1), 241-250.
- Deo, R. C., G. J. Nathan and J. C. Mi (2007). Comparison of Turbulent Jets Issuing from Rectangular Nozzles with and without Sidewalls. *Experimental Thermal & Fluid Science* 32(2), 596-606.
- Fitzgerald, J. A. and S. V. Garimella (1997). Visualization of the Flow Field in a Confined and Submerged Impinging Jet. *Proceedings of the 32th National Heat Transfer Conference*, Baltimore, MD (US), 346, 201.
- George, W. K., S. P. Capp, A. A. Seif, C. B. Baker and D. B. Taulbee (1988). A Study of the Turbulent Axisymmetric Jet. *Journal of King Saud University (Engineering Science)* 14, 85–93.
- Hussein, H. J., S. P. Capp and W. K. George (1994). Velocity Measurements in a High Reynolds Number, Momentum-Conserving, Axisymmetric, Turbulent Jet. *Journal of Fluid Mechanics* 258, 31-75.
- Jiang, F., H. Wang, Y. Wang and J. H. Xiang (2016). Simulation of Flow and Heat Transfer of Mist/Air Impinging Jet on Grinding Work-Piece. *Journal of Applied Fluid Mechanic* 9(3), 1339-1348.
- Kwon, S. J. and I. W. Seo (2005). Reynolds Number Effects on the Behaviour of a

- Nonbuoyant Round Jet. *Experiments in Fluids* 35, 801–812.
- Mickan, B. and V. Strunck (2014). A Primary Standard for the Volume Flow Rate of Natural Gas Under High Pressure Based on Laser Doppler Velocimetry. *Metrologia* 51(5), 459-475.
- Morris, G. K., S. V. Garimella and J. A. Fitzgerald (1999). Flow-Field Prediction in Submerged and Confined Jet Impingement Using the Reynolds Stress Model. *Journal of Electronic Packaging* 121(4), 255-262.
- Ötügen, M. V. (1991). Expansion Ratio Effects on the Separated Shear Layer and Reattachment Downstream of a Backward-facing Step. *Experiments in Fluids* 10(5), 273-280.
- Razinsky, E. and J. A. Brighton (1971). Confined Jet Mixing for Nonseparation Conditions. *Journal of Basic Engineering* 93(3), 333-347.
- Schlichting, H. and K. Gersten (2000). *Boundary Layer Theory*, Eighth ed. Springer, Hongkong.
- Sheen, H. J., W. J. Chen and S. Y. Jeng (1996). Recirculation Zones of Unconfined and Confined Annular Swirling Jets. *Aiaa Journal* 34(3), 572-579.
- Sheha, A. A. A., M. Nasr, M. Hosien and E. M. Wahba (2018). Computational and Experimental Study on the Water-Jet Pump Performance. *Journal of Applied Fluid Mechanics* 11(4), 1013-1020.
- So, R. M., S. A. Ahmed and H. C. Mongia (1985). Jet Characteristics in Confined Swirling Flow. *Experiments in Fluids* 3(4), 221-230.
- Suresh, P. R., K. Srinivasan, T. Sundararajan and S. K. Das (2008). Reynolds Number Dependence of Plane Jet Development in the Transitional Regime. *Physics of Fluids* 20, 044105.
- Yang, X., X. Long and X. Yao (2012). Numerical Investigation on the Mixing Process in a Steam Ejector with Different Nozzle Structures. *International Journal of Thermal Sciences* 56, 95-106.
- Zhang, H., L. Jia, L. S. Cui and C. H. Li (2019) The Development of Top-Hat Flow Field in a Circular Symmetrical Subsonic Nozzle. *Journal of Thermal Science* 28(5), 975-983.